

Supplementary Information for *Inorganic Chemistry Frontiers*.

*Perovskite photoinitiated RAFT-mediated polymerization-induced self-assembly
for organic-inorganic hybrid nanomaterials*

Bingfeng Shi^{1,2}, Wanchao Hu¹, Shiyi Li¹, Zhinan Xia¹, and Changli Lü^{*1}

¹ *Institute of Chemistry, Northeast Normal University, Changchun 130024, P. R. China*

² *Institute of Chemistry, Baotou Teachers College, Baotou 014030, P. R. China.*

* Corresponding author.

E-mail addresses: lucl055@nenu.edu.cn (C. Lü).

1 General Information of Materials and Analytical Methods	3
1.1 Materials.	3
1.2 Instrumentation and characterization.	3
2 The Summary of PQDs as photo-catalyst in photopolyziation.....	5
3 Ligand Exchange Strategy to Prepare F-PQDs : including the Supplementary Information of Figure 1.....	6
3.1 Preparation of CsPbBr ₃ PQDs.....	6
3.2 Preparation of F-PQDs.	7
3.3 Optimization of the ligand exchange conditions.....	8
3.4 Supplementary Information of Figure 1.....	9
4 PET-RAFT polymerization of PQDs and F-PQDs	11
4.1 General procedure of PQDs/F-PQDs mediated PET-RAFT polymerization.	11
4.2 Optimization of the PET-RAFT polymerization conditions.....	11
4.3 The Structural determination and calculation of the molecular weight of PFOEMA based on ¹ H NMR analysis.	12
5 PISA mediated by PET-RAFT polymerization of PQDs and F-PQDs : including the Supplementary Information of Figure 2 and Figure 3.	17
5.1 Synthesis of POEGMA-CTA.	17
5.2 Calculation of the degree of polymerization (DP) and molecular weight of POEGMA-CTA based on ¹ H NMR analysis.	18
5.3 General procedure of POEGMA-b-PFOEMA through PISA technique mediated by PQDs/F-PQDs... ..	19
5.4 Calculation of the DP and molecular weight of POEGMA ₇₈ -b-PFOEMA based on ¹ H NMR analysis.	20
5.5 Supplementary Information of Figure 2 and Figure 3	23

1 General Information of Materials and Analytical Methods

1.1 Materials.

4-Cyano-4-((phenylcarbonothioyl)thio)pentanoic acid (CPADB), 2-(perfluorooctyl)ethyl methacrylate (FOEMA), and pentadecafluorooctanoic acid (PFOA) were obtained from Shanghai Bide Reagent Co. Ltd. 1-Octadecene(90%), oleic acid (80-90%), oleylamine (80-90%), cesium bromide (CsBr, 99.5%), caesium carbonate (Cs_2CO_3 , 99.5%), lead bromide (PbBr_2 , 99%) were purchased from Aladdin Chemical Reagent Co. Ltd. Poly(ethylene glycol) monomethyl ether methacrylate ($M=500$, OEGMA, >99%) and 2,2'-azobis(2-methylpropionitrile) (AIBN) were obtained from Shanghai Macklin Reagent Co. Ltd. The inhibitors in all monomers were removed by permeation through a basic alumina column. AIBN was recrystallized with ethanol before being utilized. Other reagents are commercially available without further purification.

1.2 Instrumentation and characterization.

The molecular weight and distribution ($\text{Đ}=M_w/M_n$) of the polymer were determined by gel permeation chromatography (GPC) equipped with Waters 1515 pump and Waters 2414 differential refractive index detector, using a Styragel HT3 (7.8×300 mm) Column and a Styragel HT4 (7.8×300 mm) Column. The flow rate of the trichloromethane (30°C) eluent was 1.0 mL/min. The polymers were purified by multiple precipitations and dissolved in solvent by sonication for measurements. ^1H -NMR spectra were obtained on a 500 MHz AVANCE Bruker NMR spectrometer using deuterated CDCl_3 or $\text{CF}_2\text{ClCFCl}_2:\text{CDCl}_3$ (V: V=3:2) as solvent. X-ray diffraction (XRD) patterns were measured on a Bruker D8 Advance diffractometer using Cu Ka radiation. X-ray photoelectron spectroscopy (XPS) was performed on a USWHA 150 photoelectron spectrometer with an achromatic monochromatic light source Al Ka (1486.6 eV). PL spectra were obtained on a fluorescence

spectrophotometer (Edinburgh FLSP920). The UV-vis absorption spectra were recorded between 200 and 1100 nm using a Cary7000 UV-Vis-NIR Spectrophotometer. The LED light intensities were measured using the optical power meter (CEAULIOHT, CEL-FZ-A). All LED light sources were obtained from Xuzhou Ai Jia electronic technology Co. LTD. Transmission electron microscopy (TEM) was observed by a JEM2100F electron microscope. TEM sample was prepared by dropping 10 μ L of the colloidal solution onto the copper grid and dried at ambient temperature before observation. The topography and composition were measured by Hitachi SU8010 field-emission scanning electron microscopy (Japan) with energy dispersion X-ray spectroscopy (EDS). For SEM samples, 10 μ L of the colloidal solution was dropped onto the silicon surface and repeated three times, then dried at room temperature.

2 The Summary of photopolyzization by PQDs as photo-catalyst.

Table S1. Summary of the reported photo-catalytic polymerization of perovskite.

Literature	Materials	Monomer	Type	Application
<i>J. Am. Chem. Soc.</i> 2017 , 139, 12267 ^[1]	CsPbI ₃	PEDOT	Photo-induced redox polymerization	Photocatalytic polymerization
<i>Adv. Mater.</i> 2018 , 30, 1800774 ^[2]	CsPbBr ₃	Styrene	Surface initiated polymerization	LED
<i>ACS Macro Lett.</i> 2020 , 9, 725–730 ^[3]	CsPbBr ₃	Acrylic acid monomer	PET-RAFT polymerization	Photocatalytic polymerization
<i>J. Am. Chem. Soc.</i> 2022 , 144, 12901 ^[4]	Conjugated polymer/CsPbBr ₃ Composite	MA	Photo-ATRP	Photocatalytic polymerization
<i>ACS Energy Lett.</i> 2022 , 7, 610 ^[5]	CsPbBr ₃	MMA	PET-RAFT surface initiated photopolymerization	Photocatalytic polymerization
<i>J. Am. Chem. Soc.</i> 2022 , 144, 44, 20411 ^[6]	CsPbBr ₃	Acrylic acid monomer	PET-RAFT surface initiated photopolymerization	Photocatalytic polymerization
<i>ACS Energy Lett.</i> 2022 , 7, 4389 ^[7]	CsPbBr ₃ @MSNs Nanocomposite material ^a	Acrylic acid monomer	PET-RAFT polymerization	Photocatalytic polymerization
<i>ACS Materials Lett.</i> 2022 , 4, 464 ^[8]	Perovskite–COF Nanocomposite material	Water soluble monomer	Free radical polymerization	Photocatalytic polymerization
<i>Adv. Funct. Mater.</i> 2022 , 32, 2207655 ^[9]	Zr-MOF coated perovskite	Conjugated / unconjugated monomer	PET-RAFT polymerization	Photocatalytic polymerization
<i>Chem. Eng. J.</i> 2022 , 428, 130974 ^[10]	FAPbBr ₃	MMA	Free radical polymerization	Down conversion display film

Note: ^a CsPbBr₃ NCs is embedded in dendritic mesoporous SiO₂ (MSNs).

3 Ligand Exchange Strategy to Prepare F-PQDs : including the Supplementary Information of Figure 1.

3.1 Preparation of CsPbBr₃ PQDs.

CsPbBr₃ PQDs were synthesized according to the published literature^[11]. In a 100 mL 3-neck flask, Cs₂CO₃ (0.814 g), octadecene (40 mL), and oleic acid (2.5 mL) were added and dried for 1h at 120 °C to remove water. Then, the mixture was heated under N₂ to 150 °C until all Cs₂CO₃ reacted with OA. Since Cs-oleate precipitates out of ODE at room temperature, it has to be pre-heated to 100 °C before injection.

In the next step, ODE (10 mL) and PbBr₂ (0.138g) were loaded into a 25 mL 3-neck flask and dried under vacuum for 1h at 120 °C. Dried oleylamine (1 mL, OLA) and dried OA (1 mL) were injected in 1h at 120 °C under N₂. After PbBr₂ dissolved, the temperature was raised to 180 °C and Cs-oleate solution (1 mL, prepared as described above) was quickly injected and, 5s later, the reaction mixture was cooled by the ice-water bath. The solution was transferred to the 50 mL centrifuge tube and added 10 mL acetone. The mixture was centrifuged at 10000 rpm for 5 min to obtain precipitation. The precipitation redissolved in toluene and centrifuged at 3500 rpm for 5 min to gather supernatant. Take 1 mL of the supernatant, dry it under vacuum and weigh it, then dilute the supernatant to 8mg.mL⁻¹ and stored in dark environment.

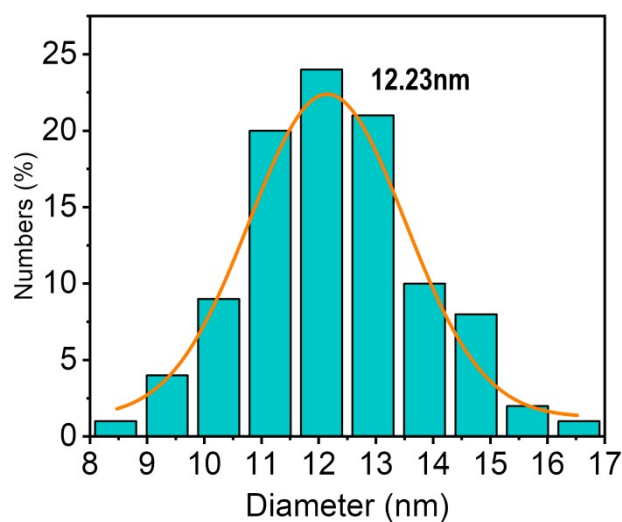


Figure S1. Size-distribution histogram of PQDs

3.2 Preparation of F-PQDs.

In a typical experiment^[12], CsPbBr₃ PQDs toluene solution (8 mg·mL⁻¹, 10 mL) and PFDA (2.4 mg) were added in a 25 mL three-neck round-bottomed flask under an N₂ atmosphere. Then, the mixture was stirred for 1 h in the dark and stored for further utilization. Among them, the mass ratio of PFDA to PQDs is 3:100.

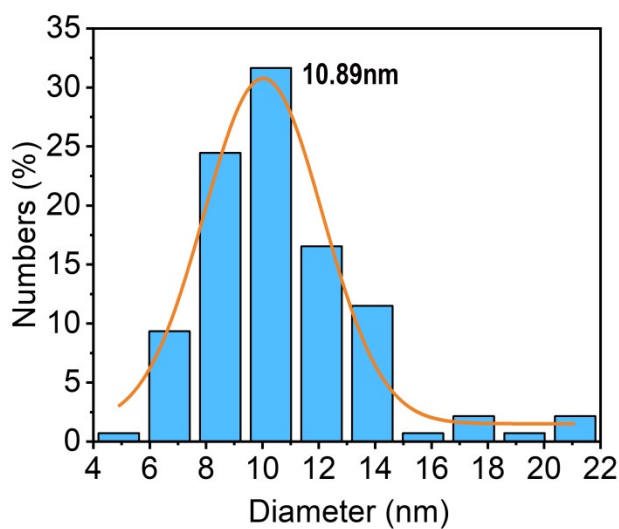


Figure S2. Size-distribution histogram of F-PQDs.

3.3 Optimization of the ligand exchange conditions.

In the initial experimental exploration, we carried out a series of adjustment experiments on the addition amount of PFOA. During the monitoring of the experimental phenomenon, we found that when the addition amount of PFOA exceeded 10% of the perovskite mass, the fluorescence in the system would be quenched and an orange precipitate formed quickly. When the mass ratio of PFOA in the system was greater than 5%, although the fluorescence intensity was still enhanced, larger particles of perovskite nanoparticles would be formed during storage to form precipitation. When the addition amount of PFOA was 1%, the enhancement of fluorescence intensity was limited (Figure S3).

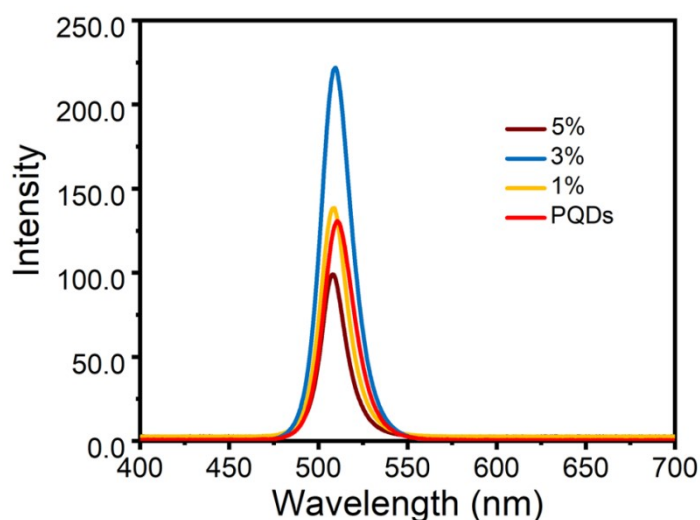


Figure S3. PL spectra of PQD's colloidal solutions obtained by different feeding amount of PFOA.

3.4 Supplementary Information of Figure 1

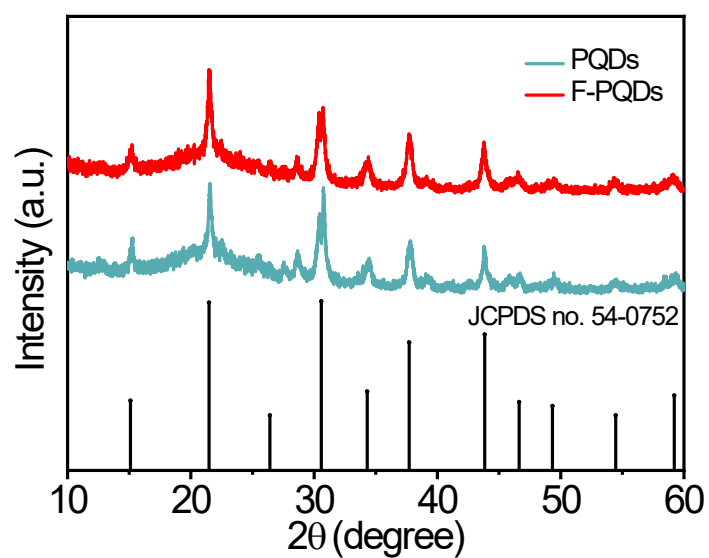


Figure S4. XRD spectra of PQDs and F-PQDs, and standard XRD patterns of CsPbBr₃.

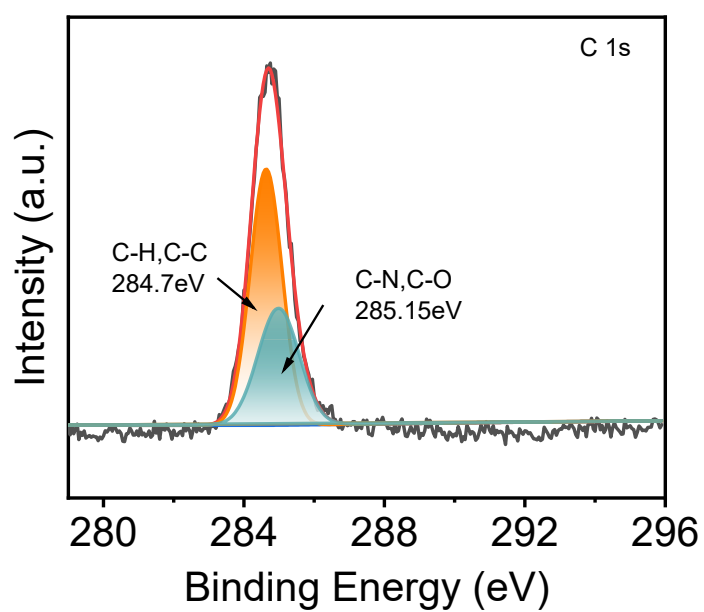


Figure S5. High-resolution C 1s spectra of PQDs.

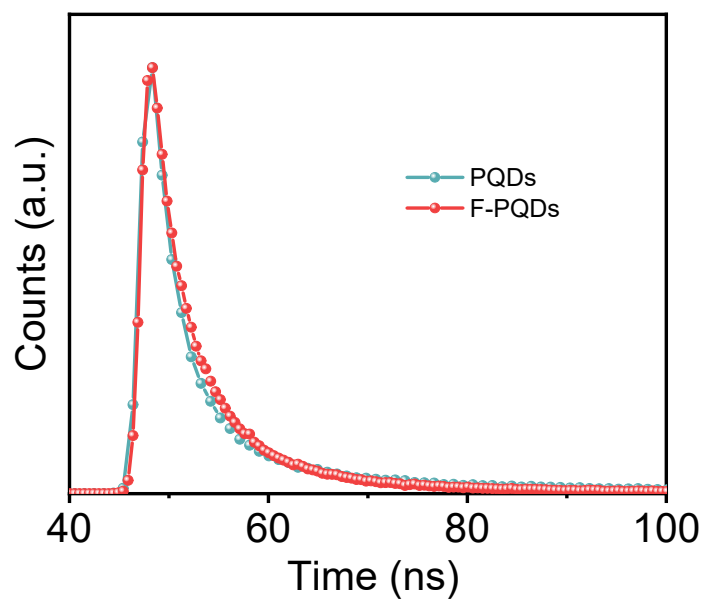


Figure S6. Time-resolved FL decay curves of PQDs and F-PQDs.

Table S2. Summary of PLQY and time-resolved FL decay measurements, where the lifetimes of samples were tested in toluene solution. τ_{ave} is the average decay lifetimes. τ_1 and τ_2 are the detailed recombination lifetimes, and A and B represent the ratio of component contribution to the decay.

Samples	$\tau_1(\text{ns})$	A%	$\tau_2(\text{ns})$	B%	$\tau_{\text{ave}}(\text{ns})^a$	χ^2	PLQY
PQDs	3.06	40.16	12.75	59.86	11.41	1.28	48
F-PQDs	3.60	50.47	10.63	49.53	8.83	1.18	73

a : The mean lifetime τ_{ave} is calculated by the Equation S1:

$$\tau_{\text{ave}} = \frac{A * \tau_1^2 + B * \tau_2^2}{A * \tau_1 + B * \tau_2} \quad (\text{S1})$$

4 PET-RAFT polymerization of PQDs and F-PQDs

4.1 General procedure of PQDs/F-PQDs mediated PET-RAFT polymerization.

In a typical experiment, FOEMA (0.5 g, 0.94 mmol), CPADB (2.6 mg, $9.4 \times 10^{-5} \text{ mol} \cdot \text{L}^{-1}$), 62.5 μL PQDs/F-PQDs solutions were loaded into a 25 mL 3-neck flask, then 10 g toluene was added in the mixture. The mixture was stirred for 1 h at room temperature under an N_2 atmosphere. Then, the mixture was photopolymerized under LED light ($\lambda = 425 \text{ nm}$, $5 \text{ mW}/\text{cm}^2$) for 12 h. The reaction was quenched in liquid nitrogen, and the product was purified by precipitation in hexane and centrifugation. The precipitation was washed with hexane three times, and the product was dried under vacuum. In this process, the molar ratio of [monomer]: [CPADB] is 100:1 and the amount of PC was the 1% of monomer mass. Furthermore, the mass ratio of solvent to monomer is 20: 1.

4.2 Optimization of the PET-RAFT polymerization conditions.

Table S3. Optimization of polymerization condition.

Entry	Light source ^a	[M] : [CTA]	PC (wt%)	t (h)	Conv.(%) ^b	M_{nNMR} (kDa) ^b
1	365 nm	100:1	-	12	Trace	-
2	365 nm	100:1	1	12	11.2	6.2
3	365 nm	100:1	1	12	10.6	5.9
4	425 nm	100:1	-	12	Trace	-
5	425 nm	100:1	1	12	18.3	10.0
6	425 nm	100:1	1	12	26.2	14.2
7	425 nm	100:1	1	18	25	13.6
8	425 nm	100:1	1	18	28	15.2

9	425 nm	100:1	1	24	25	13.6
10	425 nm	100:1	1	24	28	15.2
11	465 nm	100:1	-	12	-	-
12	465 nm	100:1	1	12	10.3	12.5
13	465 nm	100:1	1	12	10.6	13.6

^aAll photopolymerization experiments were carried out under the irradiation of LED lamps. The optical density of 365 nm LED light was 2 mW/cm², and the optical density of other lamps was 5 mW/cm².

^bThe conv. (%) and M_n (kDa) were determined by ¹H NMR.

On the basis of referring to previous literature, we screened LED light sources based on polymerization efficiency and fluorescence emission intensity. In the initial experiment process, we found that the maximum optical density of the 365 nm LED lamp can only reach 2 mW/cm², and the fluorescence intensity decreases during the actual experiment process. Under the same time of 425 nm and 465 nm light sources, the conversion rate of the polymer under 425 nm light source is higher, so in the following experiments we all used 425 nm light source for photopolymerization

4.3 The Structural determination and calculation of the molecular weight of PFOEMA based on ¹H NMR analysis.

The structure of polymer **PFOEMA** and the molecular weight were determined by ¹H-NMR spectra. The signals at 7.30–8.0 ppm can be attributed to the protons of the benzene ring in CPADB. Signals at 5.79 and 5.25 ppm can be attributed to the protons of the –CH=CH– on oleic acid and oleylamine, respectively. The broad signal d at 4.2 ppm is ascribed to the methylene hydrogen which is connected to the fluorocarbon chain of FOEMA. Signal c at 2.53 ppm is assigned to the –CH₂– connected to methacrylate group in FOEMA. The methine and methylene proton

peaks at 0.8–2.0 ppm are attributed to signals a and b in the backbone of the polymer main chain. As shown in the Figure S7, the integration areas of signal d can represent the numbers of the FOEMA and the integration areas of signal e, f, and g can represent the numbers of the CPADB. Based on the spectra, the molecular weight PFOEMA is calculated according to Equation S2 :

$$M_{n\text{ NMR}} = M_{n(\text{FOEMA})} \frac{[d]/2}{[e, f, g]/5} + M_{n(\text{CPADB})} \quad (\text{S2})$$

$M_{n(\text{FOEMA})}$ is the molecular weight of the FOEMA and the $M_{n(\text{CPADB})}$ is the molecular weight of CPADB.

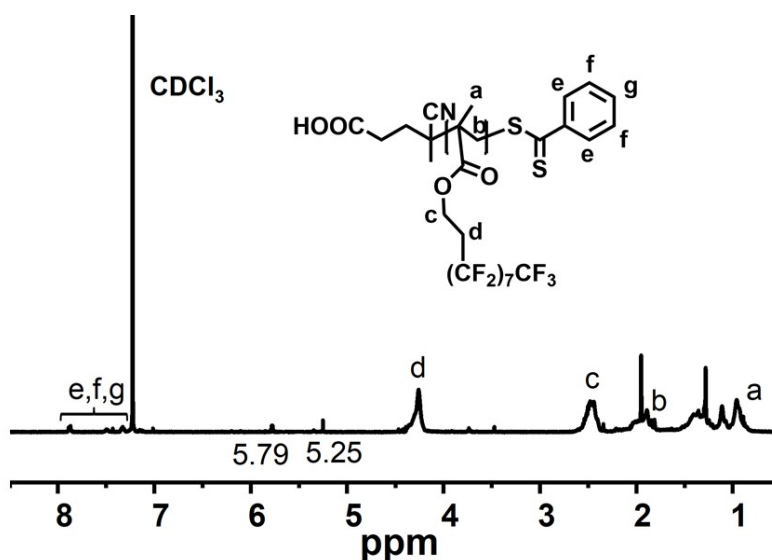


Figure S7. Representative ¹H NMR spectrum of PFOEMA.

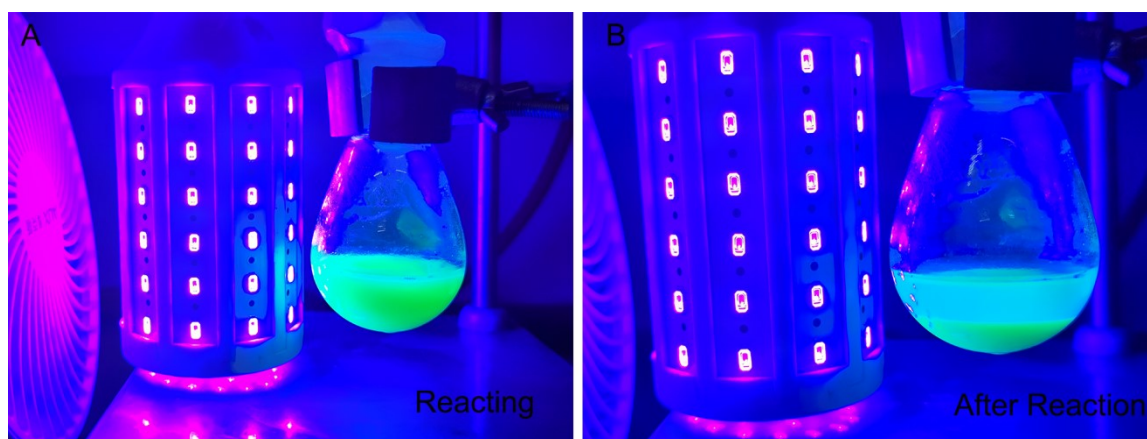


Figure S8. Photographs of PET-RAFT polymerization process by PQDs.

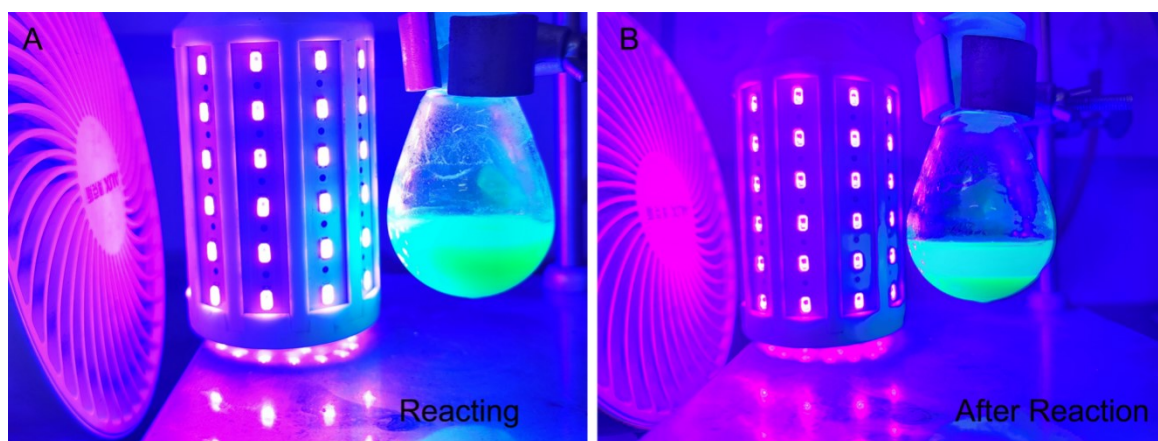


Figure S9. Photographs of PET-RAFT polymerization process by F-PQDs.

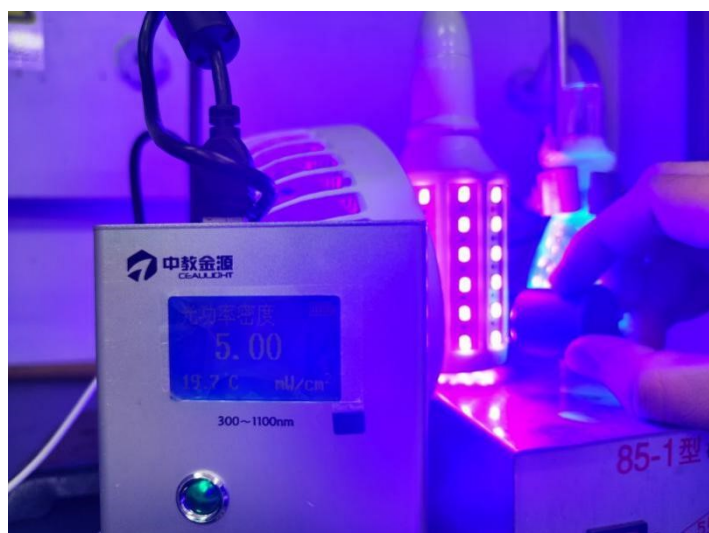


Figure S10. Photographs of optical density detection process.

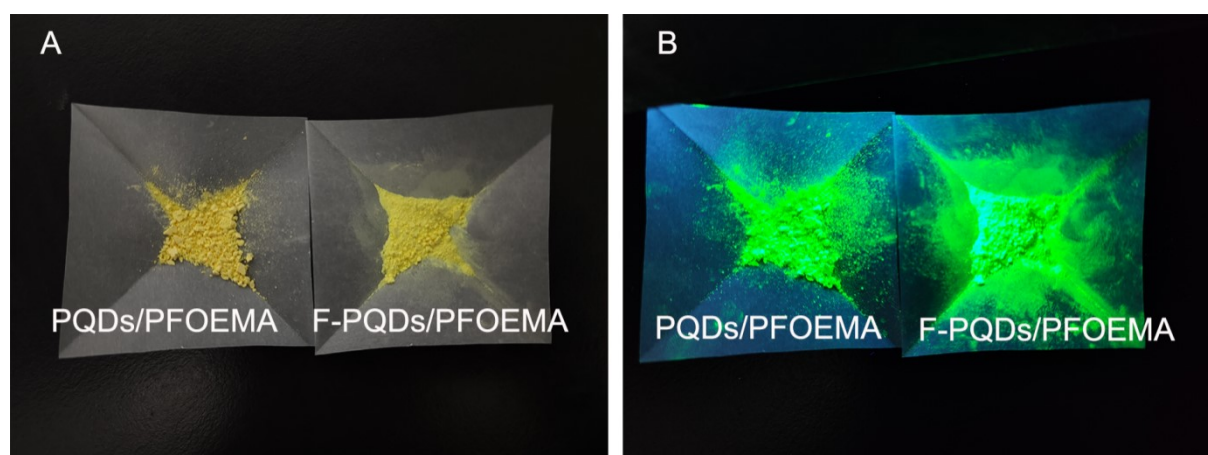


Figure S11. Photographs of PQDs/PFOEMA and F-PQDs/PFOEMA composites in daylight and 365 nm light.

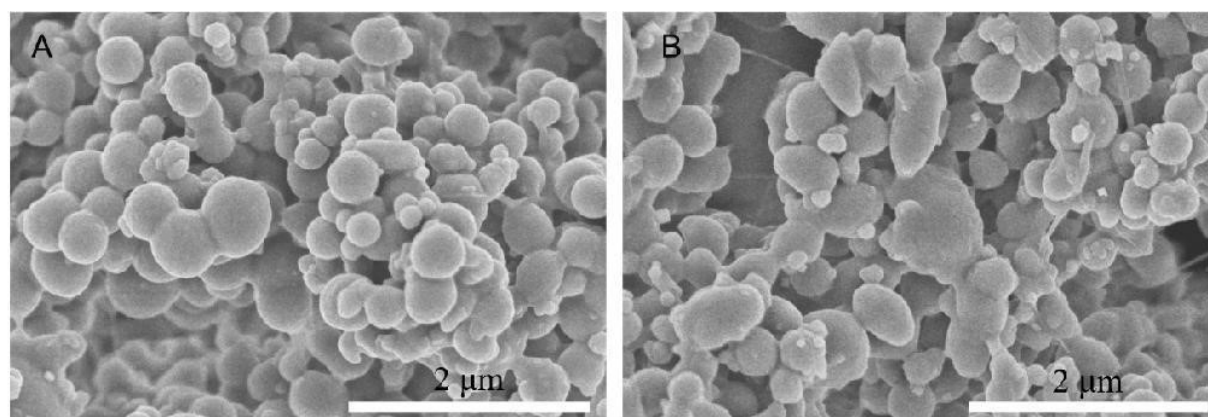


Figure S12. SEM images of PQDs/PFOEMA and F-PQDs/PFOEMA composites.

5 PISA mediated by PET-RAFT polymerization of PQDs and F-PQDs : including the Supplementary Information of Figure 2 and Figure 3.

5.1 Synthesis of POEGMA-CTA.

In a typical experiment, OEGMA (20 g, 0.04 mol), CPADB (0.15 g, 0.53 mmol), AIBN (0.044 g, 0.265 mmol) and THF (20 mL) were added to a 100 mL three-neck round-bottomed flask. After three freeze–pump–thaw cycles in an N₂ atmosphere, the mixture was stirred at 70 °C for 12 h. Then, the reaction was quenched in liquid nitrogen, and the product was purified by precipitation in ether and centrifugation. After repeating this procedure three times, the product was dried under vacuum. The Mn of POEGMA-CTA determined by GPC was 39.9 kDa with a narrow polydispersity index ($D= 1.18$) (Figure S1†).

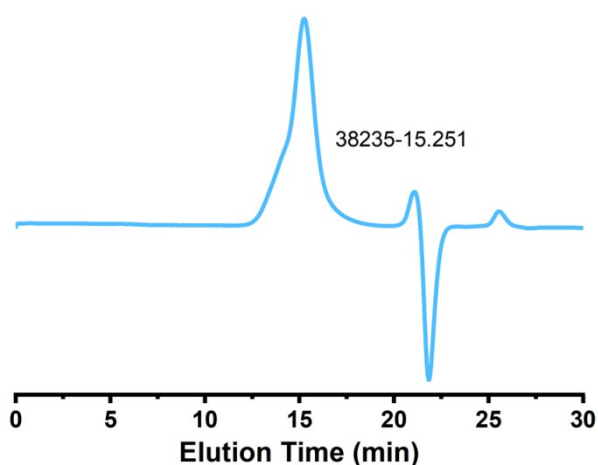


Figure S13. GPC trace of POEGMA-CTA.

5.2 Calculation of the degree of polymerization (DP) and molecular weight of POEGMA-CTA based on ^1H NMR analysis.

The structure of polymer POEGMA-CTA and the molecular weight can be determined by ^1H -NMR spectra. The signals at 7.30–8.0 ppm can be attributed to the protons of the benzene ring in CPADB. The broad signal c at 4.1 ppm is ascribed to the methylene hydrogen which is connected to the methacrylate group in OEGMA. Signal d at 3.67 ppm is assigned to the $-\text{CH}_2-$ in PEG segment. The broad signal e at 3.4 ppm is ascribed to the ether methyl hydrogen in OEGMA. The methine and methylene proton peaks at 0.8–2.0 ppm are attributed to signals a and b in the backbone of the polymer main chain. As shown in the Figure S13, the integration areas of signal c can represent the numbers of the OEGMA and the integration areas of signal e, f, and g can represent the numbers of the CPADB. Based on the spectra, the degree of polymerization (DP) of POEGMA-CTA is calculated according to Equation S3 and the molecular weight PFOEMA is calculated according to Equation S4:

$$DP = \frac{[c]/2}{[f, g, i]/5} \quad (\text{S3})$$

$$M_{n \text{ NMR}} = M_{n(\text{OEGMA})} \frac{[c]/2}{[e, f, i]/5} + M_{n(\text{CPADB})} \quad (\text{S4})$$

$M_{n(\text{OEGTMA})}$ is the molecular weight of the PEGMA and the $M_{n(\text{CPADB})}$ is the molecular weight of the CPADB. Through the calculation, we found that the DP of POEGMA-CTA is 78 and the $M_{n \text{ NMR}}$ is 39300, which is basically consistent with the results of GPC.

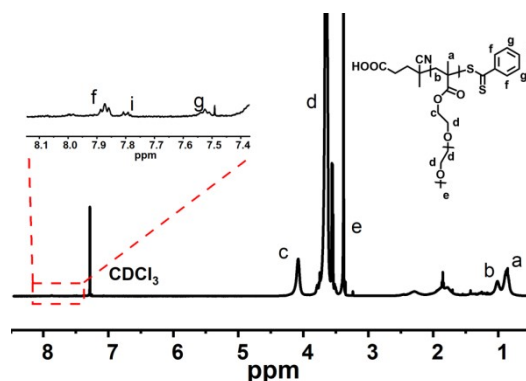


Figure S14. ^1H NMR spectra of POEGMA-CTA.

5.3 General procedure of POEGMA-b-PFOEMA through PISA technique mediated by PQDs/F-PQDs.

In a typical experiment, FOEMA (0.5 g, 0.94 mmol), POEGMA₇₈-CTA (0.37 g, 9.4×10^{-5} mol·L⁻¹), 62.5 μL PQDs/F-PQDs solutions were loaded into a 25 mL 3-neck flask, then 10 g toluene was added in the mixture. The mixture was stirred for 1 h at room temperature under an N₂ atmosphere. Then, the mixture was stirred and photopolymerized under LED light ($\lambda = 425$ nm, 5 mW/cm²) for 12 hours. The reaction was quenched in liquid nitrogen, and the product was purified by precipitation in hexane and centrifugation. The precipitation was washed with hexane three times, and the product was dried under vacuum. In this process, the molar ratio of [monomer]:[CTA] is 100:1 and the amount of PC was the 1% of monomer mass. Furthermore, the mass ratio of solvent to monomer is 10: 1.

5.4 Calculation of the DP and molecular weight of POEGMA₇₈-b-PFOEMA based on ¹H NMR analysis.

The DP of polymer POEGMA₇₈-b-PFOEMA and the molecular weight can be determined by ¹H-NMR spectra. The signals f at 4.25 ppm can be attributed to the methylene hydrogen which is connected to the methacrylate group in FOEMA. The broad signal g at 2.45 ppm is ascribed to the methylene hydrogen which is connected to the methacrylate group in FOEMA. Based on the spectra, the degree of polymerization (DP) of PFOEMA is calculated according to Equation S5 and the molecular weight PFOEMA is calculated according to Equation S6:

$$DP = \frac{[c, f] / 2 - [g] / 3}{[h, i, j] / 5} \quad (S5)$$

$$M_{n \text{ NMR}} = M_{n(\text{FOEMA})} \frac{[c, f] / 2 - [g] / 3}{[h, i, j] / 5} + M_{n(\text{POEGMA})} \quad (S6)$$

$M_{n(\text{FOEMA})}$ is the molecular weight of the FOEMA and the $M_{n(\text{POEGMA})}$ is the molecular weight of the POEGMA₇₈-CTA.

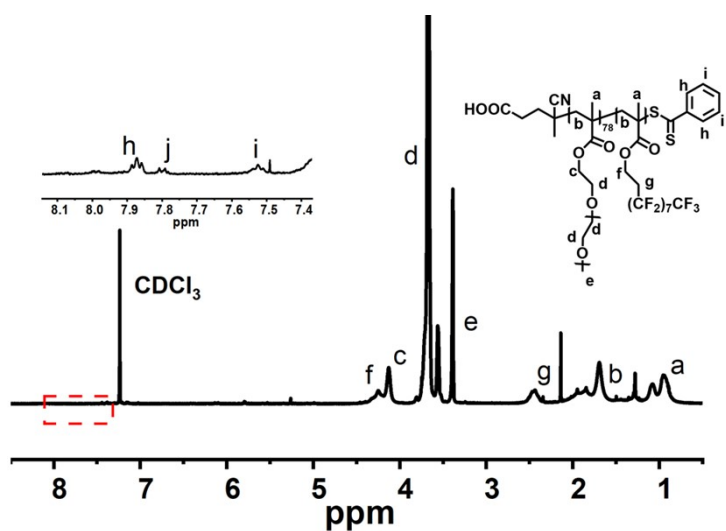


Figure S15. Representative ¹H NMR spectra of POEGMA₇₈-b-PFOEMA

Table S4. Comparison of PISA polymerization of FOEMA with different PC.

Entry	PC	[M] : [CTA]	Time (h)	Totally solid content (wt%)	Conv. (%)	M _n NMR(kDa)
1	-	100:1	24	10	-	-
2	PQDs	100:1	24	10	45	63.2
3	F-PQDs	100:1	24	10	52	66.9

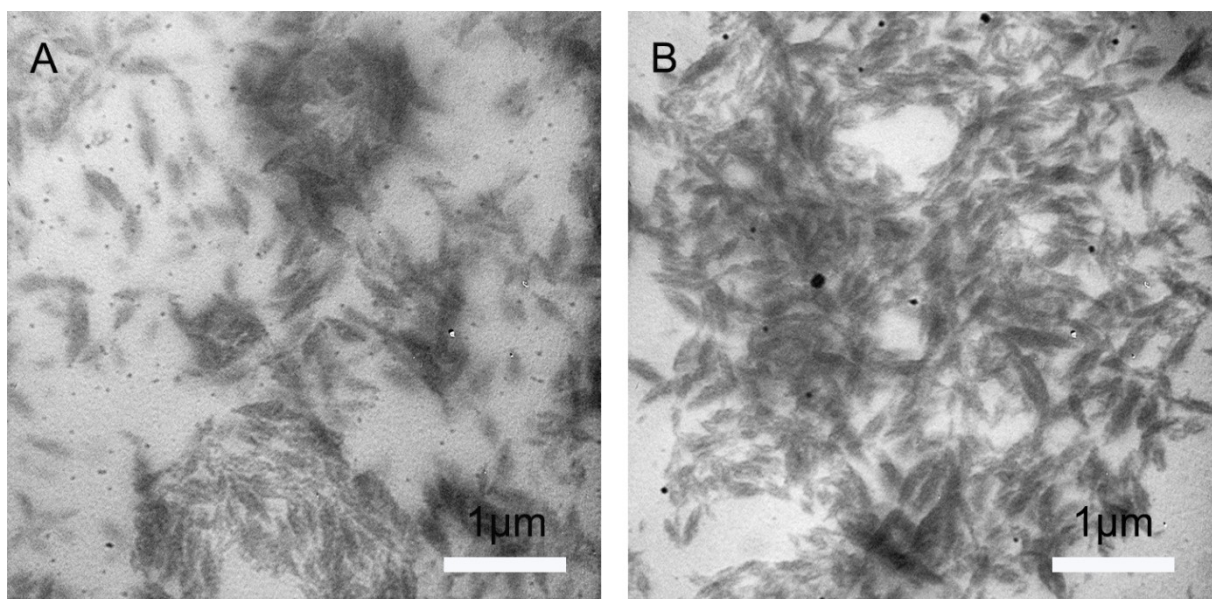


Figure S16. TEM images of self-assembled POEGMA₇₈-b-PFOEMA hybrid nano assemblies (Table S3, Entry 2 and 3).

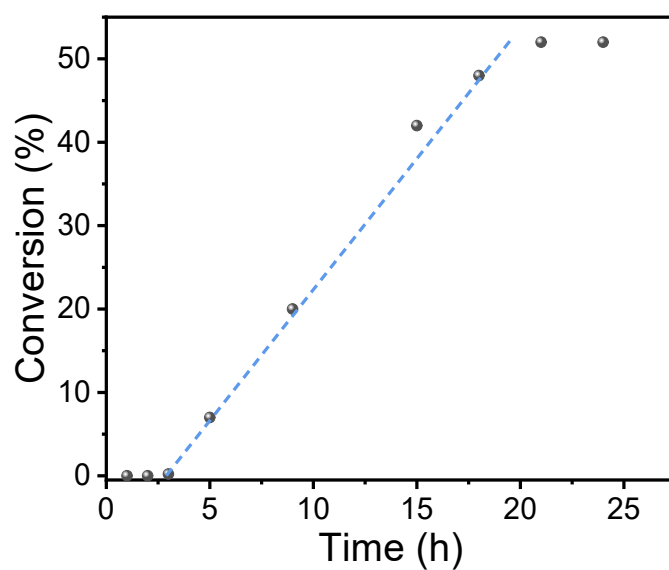


Figure S17. Monomer conversion evolution of PET-RAFT polymerization monitored by ^1H NMR. Polymerizations were performed in toluene using $[\text{FOEMA}]/[\text{POEGMA}] = 100:1$ at a total solid content of 10 wt% with 1 wt% of F-PQDs.

Table S5. PISA of $\text{POEGMA}_{78}\text{-b-PFOEMA}$ with different DPs.

Entry	PC	[M]:[CTA]	Time (h)	Totally solid content (wt%)	Conv. (%)	DP	M_{nNMR} (kDa)
1	F-PQDs	100:1	18	10	34	34	89.7
2	F-PQDs	200:1	18	10	37.5	75	100.9
3	F-PQDs	300:1	18	10	45.6	137	112.2
4	F-PQDs	400:1	24	10	53.7	215	153.7

5.5 Supplementary Information of Figure 2 and Figure 3

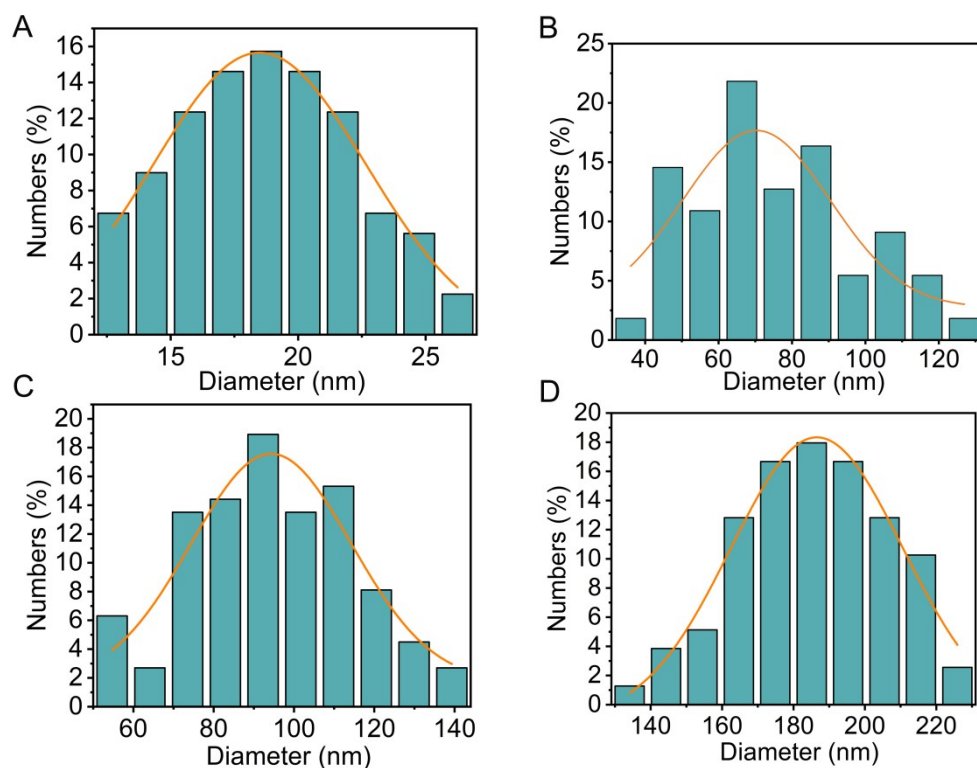


Figure S18. Size-distribution histogram of A) POEGMA₇₈-b-PFOEMA₃₄, B) POEGMA₇₈-b-PFOEMA₇₅, C) POEGMA₇₈-b-PFOEMA₁₃₇, and D) POEGMA₇₈-b-PFOEMA₂₁₅ hybrid nano assemblies based on the TEM images in Figure 3.

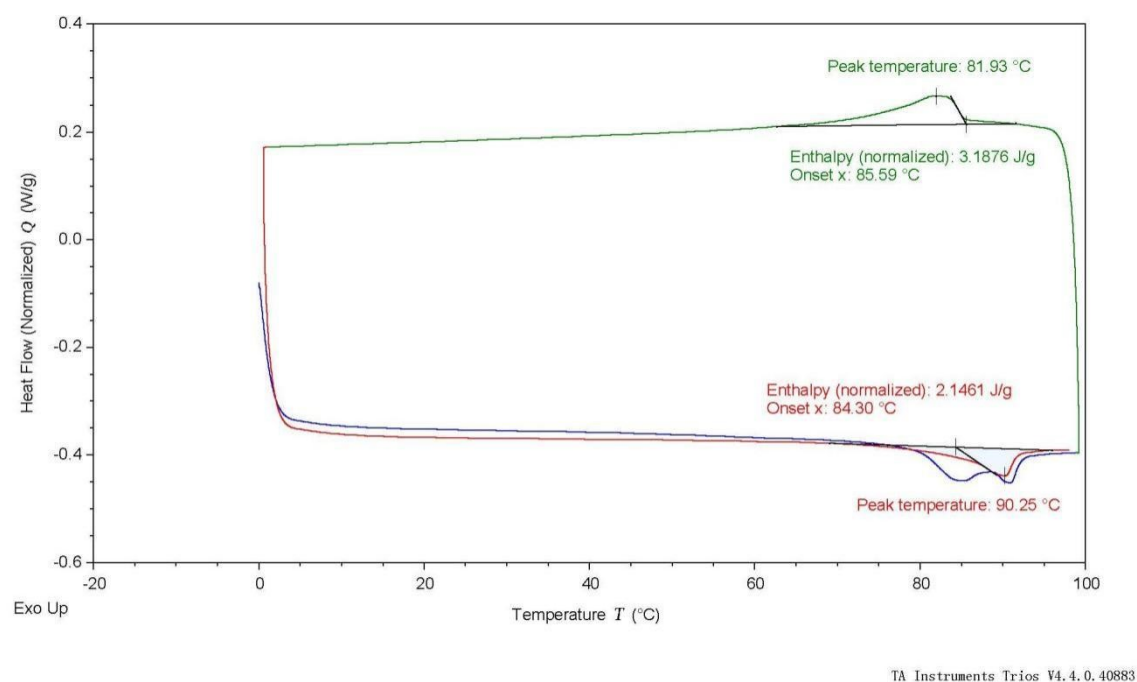


Figure S19. DSC curves of POEGMA₇₈-b-PFOEMA₃₄.

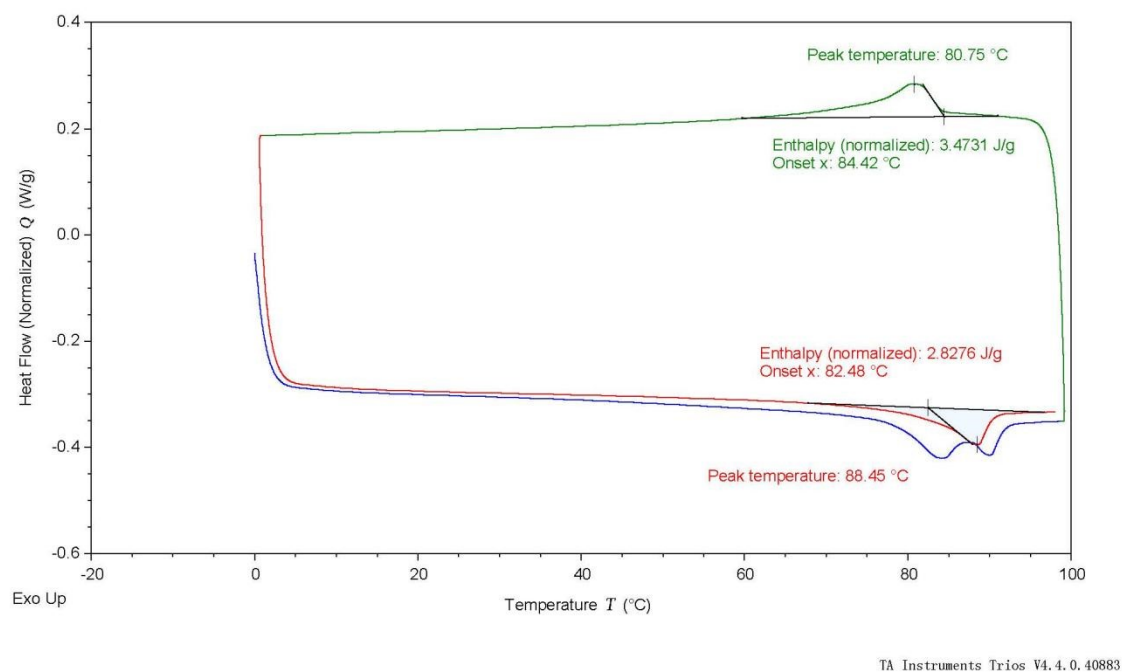
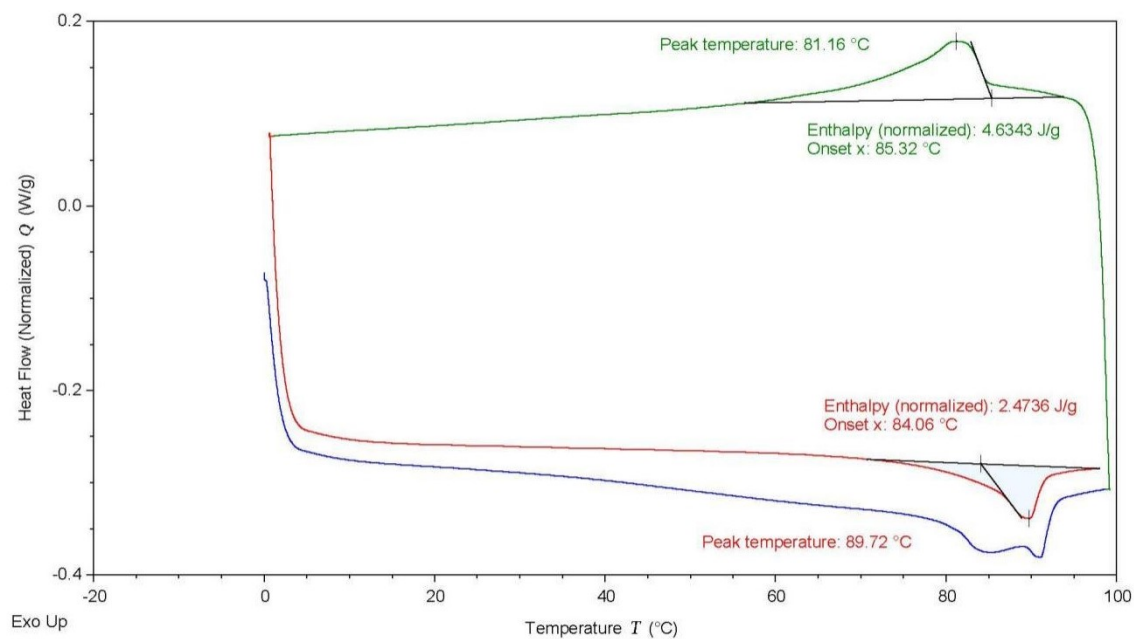
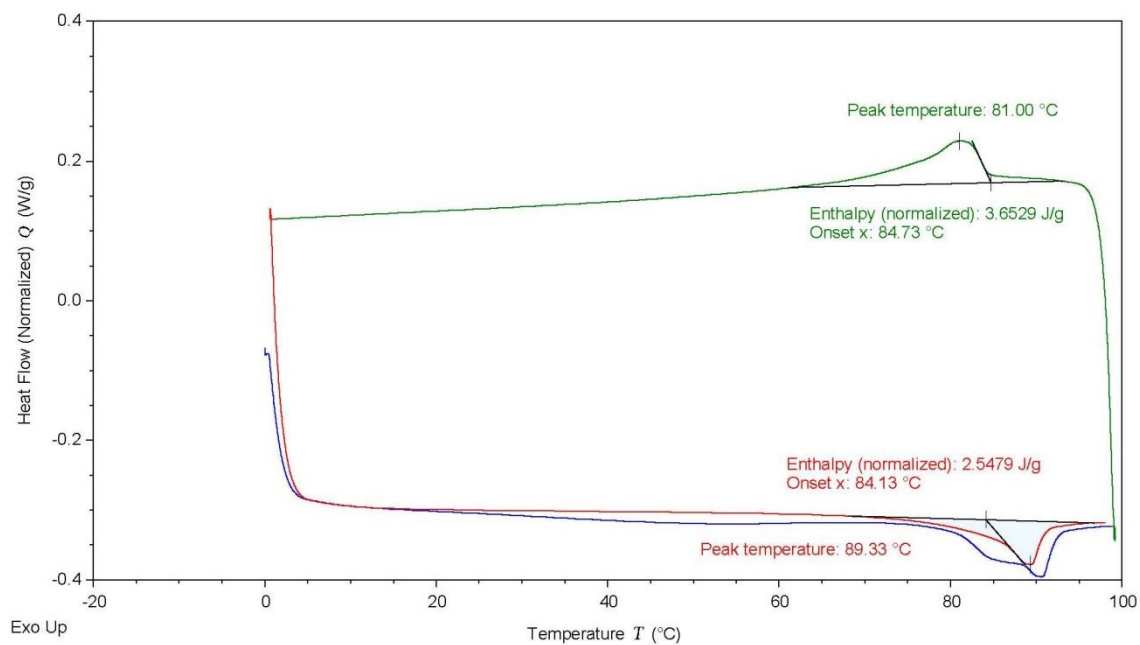


Figure S20. DSC curves of POEGMA₇₈-b-PFOEMA₇₅.



TA Instruments Trios V4.4.0.40883

Figure S21. DSC curves of POEGMA₇₈-b-PFOEMA₁₃₇.



TA Instruments Trios V4.4.0.40883

Figure S22. DSC curves of POEGMA₇₈-b-PFOEMA₂₁₅.

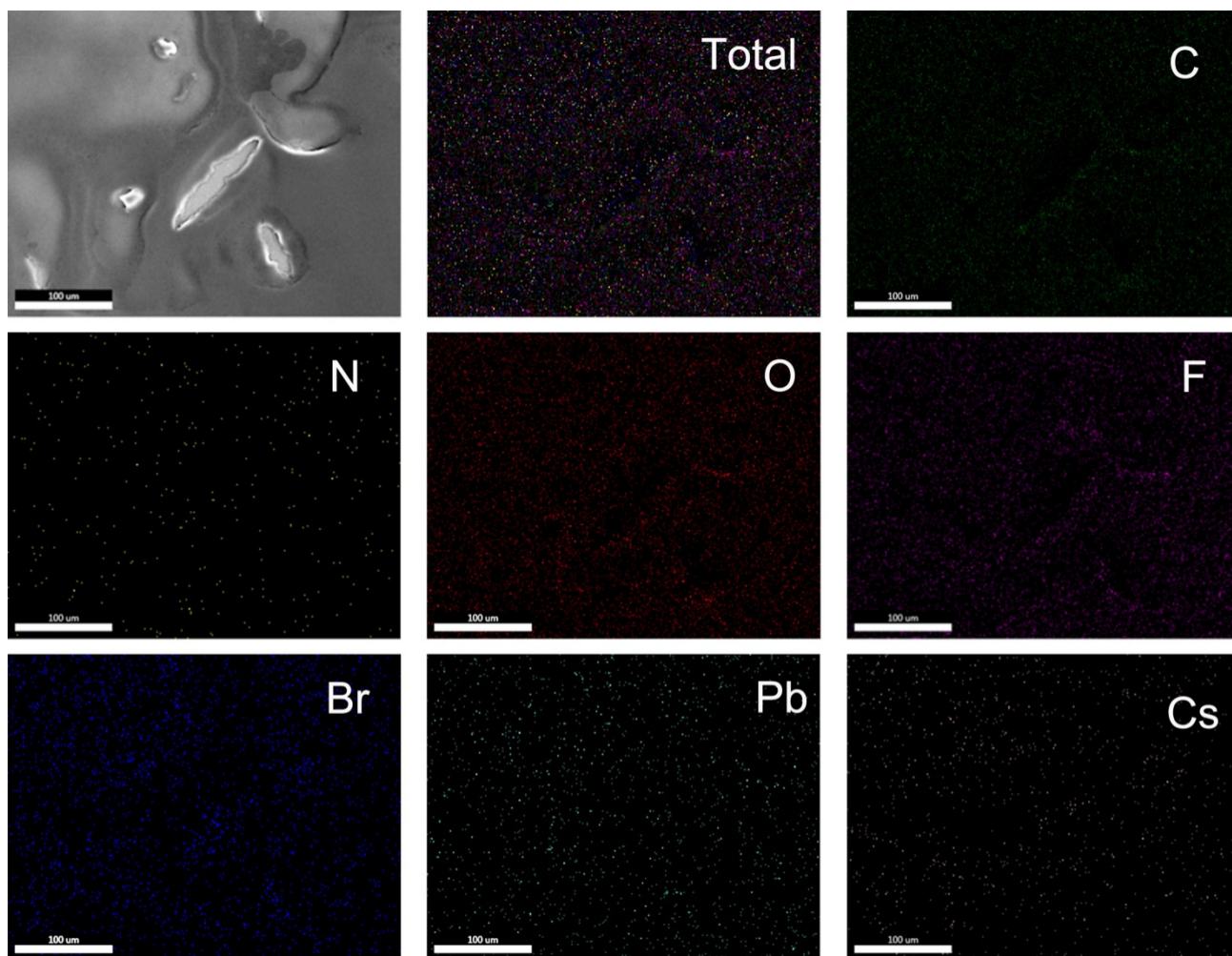


Figure S23. Elemental mapping of POEGMA₇₈-b-PFOEMA₃₄ hybrid nano assemblies. Sample preparation: 2 mL of the reaction solution was precipitated into n-hexane, washed three times with n-hexane and re-dispersed in toluene. Then, 10 μ L of the colloidal solution was dropped onto the silicon surface and repeated three times, then dried at room temperature.

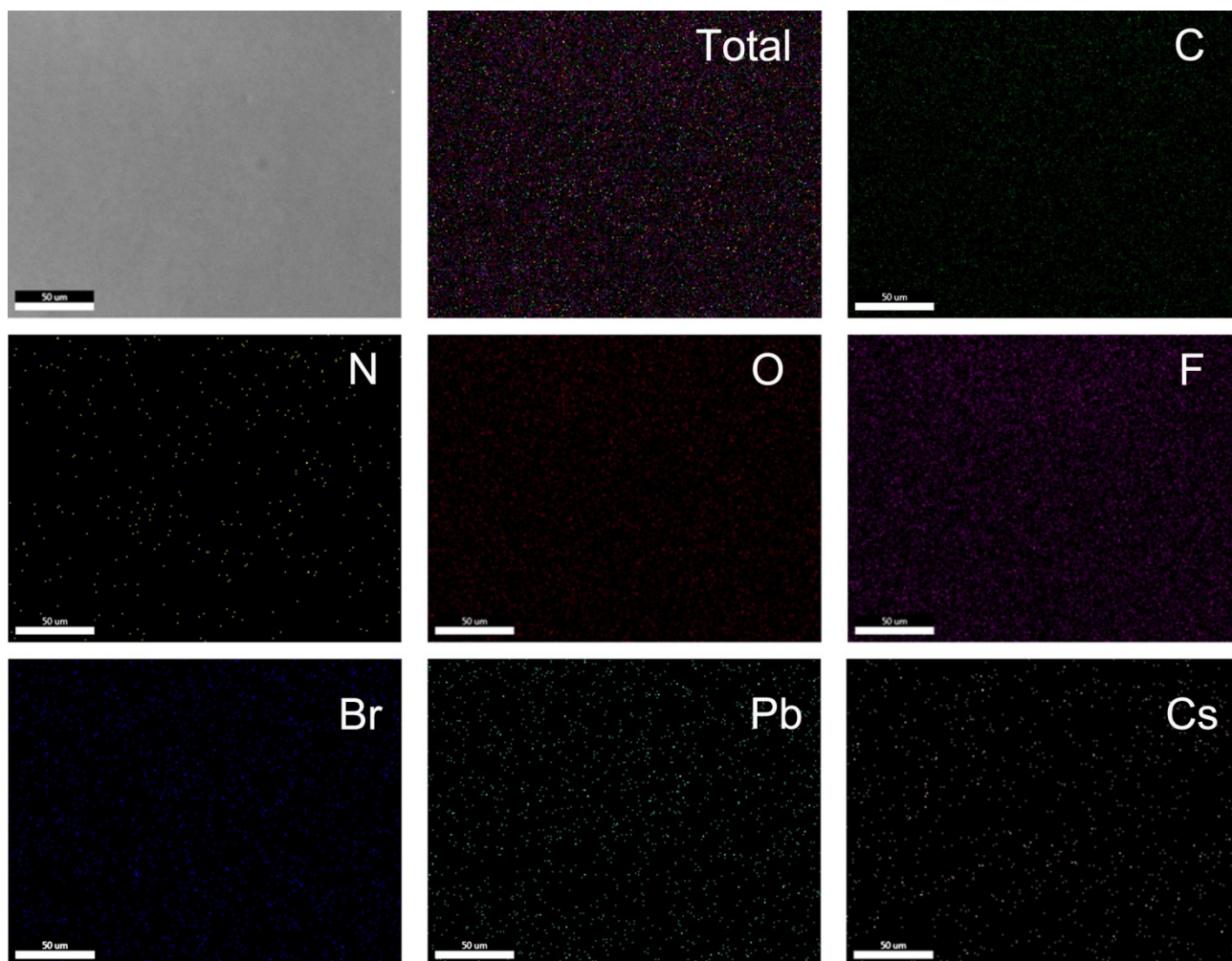


Figure S24. Elemental mapping of POEGMA₇₈-b-PFOEMA₇₅ hybrid nano assemblies. Sample preparation: 2 mL of the reaction solution was precipitated into n-hexane, washed three times with n-hexane and re-dispersed in toluene. Then, 10 μ L of the colloidal solution was dropped onto the silicon surface and repeated three times, then dried at room temperature.

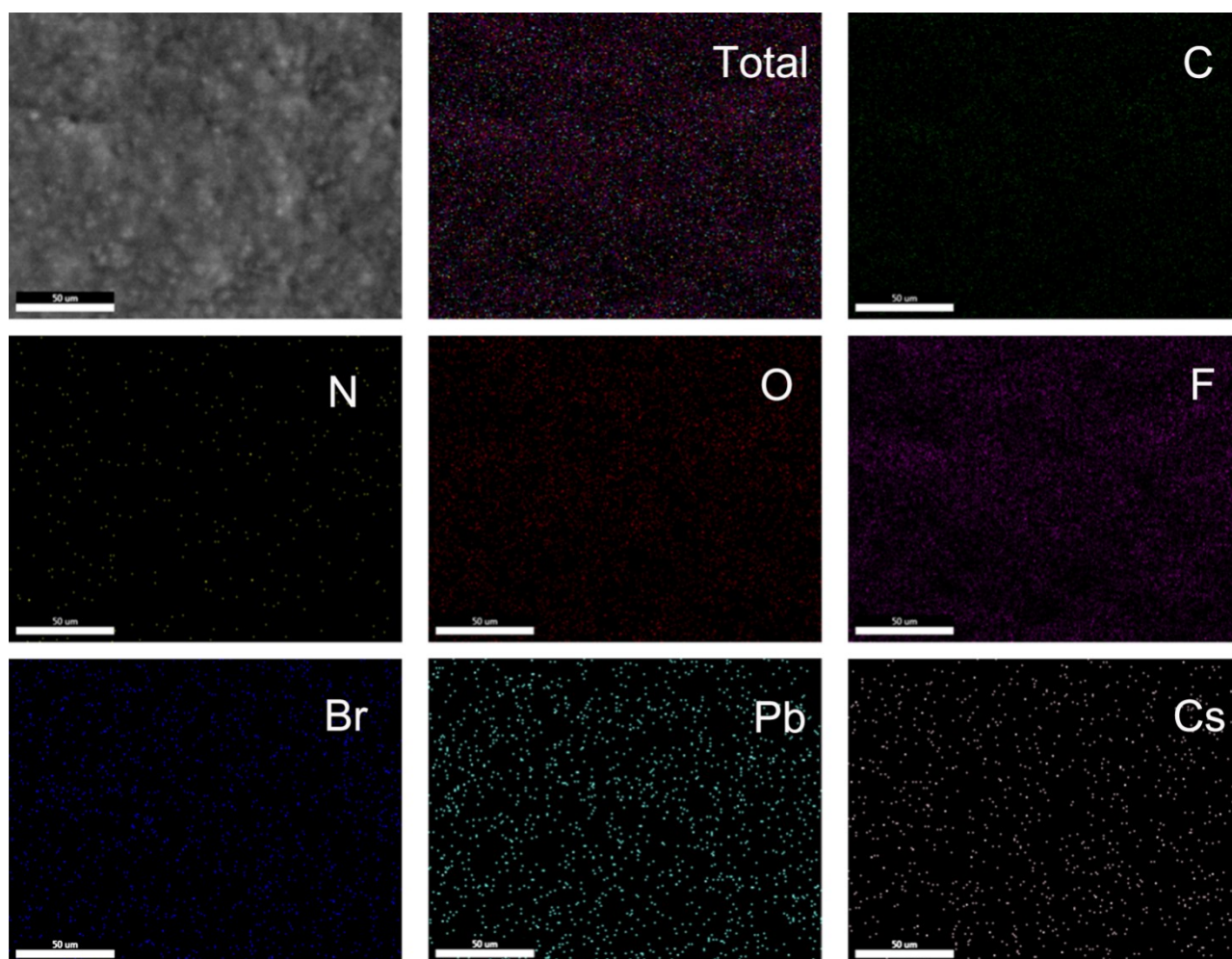


Figure S25. Elemental mapping of POEGMA₇₈-b-PFOEMA₁₃₇ hybrid nano assemblies. Sample preparation: 2 mL of the reaction solution was precipitated into n-hexane, washed three times with n-hexane and re-dispersed in toluene. Then, 10 μ L of the colloidal solution was dropped onto the silicon surface and repeated three times, then dried at room temperature.

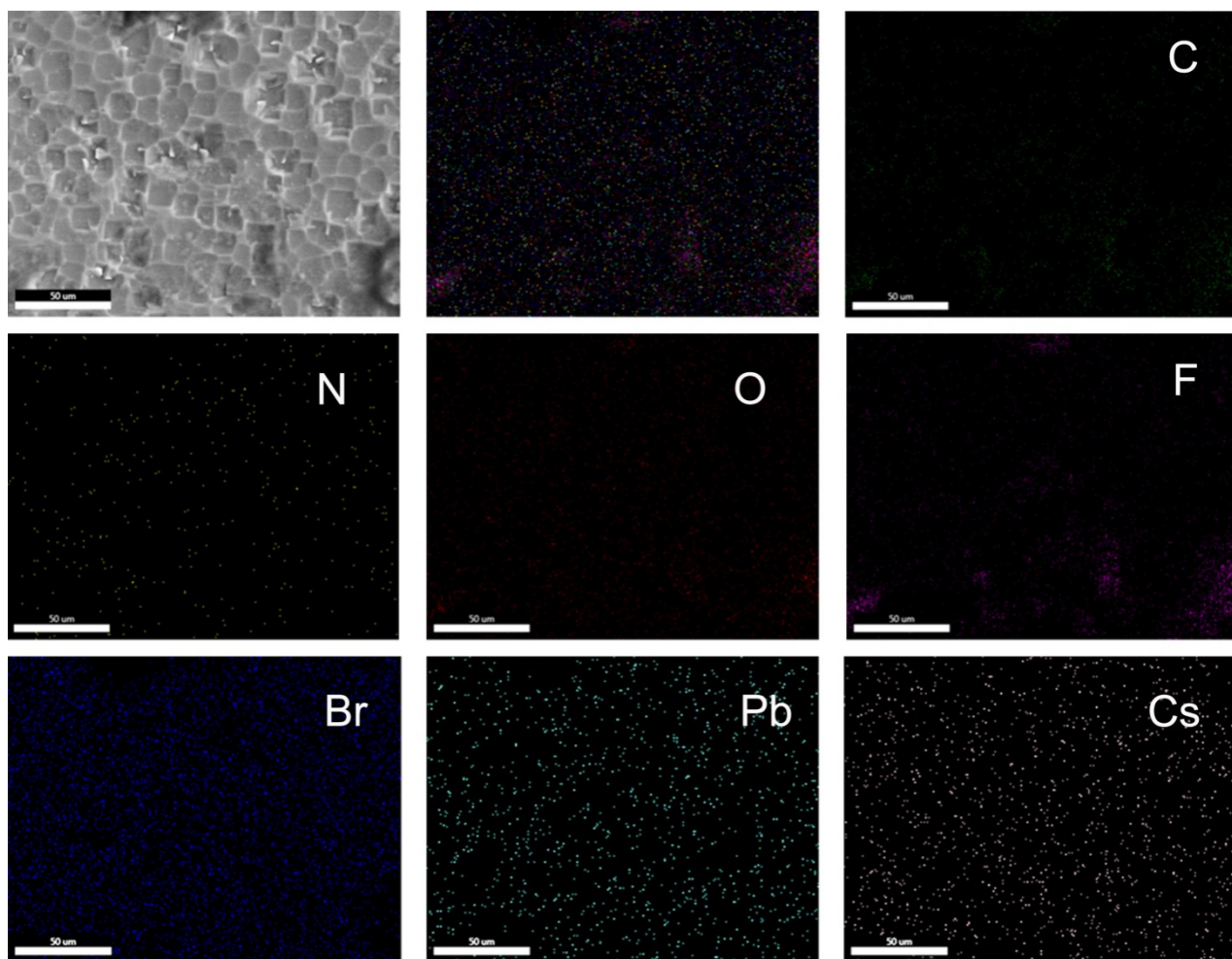


Figure S26. Elemental mapping of POEGMA₇₈-b-PFOEMA₂₁₅ hybrid nano assemblies. Sample preparation: 2 mL of the reaction solution was precipitated into n-hexane, washed three times with n-hexane and re-dispersed in toluene. Then, 10 μ L of the colloidal solution was dropped onto the silicon surface and repeated three times, then dried at room temperature.

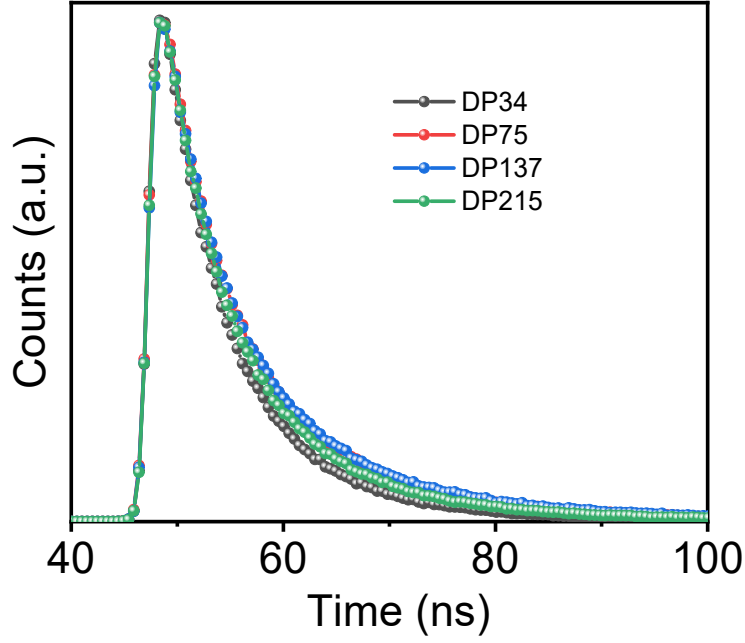


Figure S27. Time-resolved FL decay curves of different hybrid nano assemblies.

Table S6. Summary of PLQY and time-resolved FL decay measurements, where the lifetimes of samples were tested in toluene solution. τ_{ave} is the average decay lifetimes. τ_1 and τ_2 are the detailed recombination lifetimes, and A and B represent the ratio of component contribution to the decay.

Samples	$\tau_1(\text{ns})$	A%	$\tau_2(\text{ns})$	B%	$\tau_3(\text{ns})$	C%	$\tau_{\text{ave}}(\text{ns})^a$	χ^2	PLQY
DP34	4.93	45.67	9.76	49.33	29.24	5.00	17.25	1.096	26
DP75	5.62	43.21	12.75	51.44	39.11	5.34	16.08	1.028	32
DP137	5.80	41.32	13.56	52.86	46.40	5.82	19.28	1.063	31
DP215	5.23	40.76	11.32	54.54	38.49	4.70	14.89	1.092	25

a : The mean lifetime τ_{ave} is calculated by the Equation S7:

$$\tau_{\text{ave}} = \frac{A * \tau_1^2 + B * \tau_2^2 + C * \tau_3^2}{A * \tau_1 + B * \tau_2 + C * \tau_3} \quad (\text{S7})$$

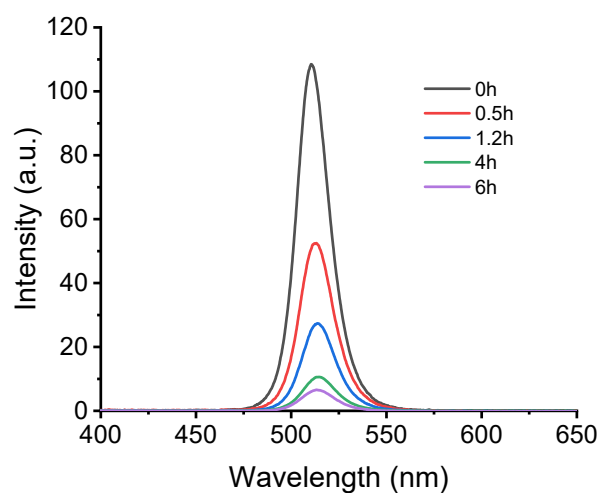


Figure S28. PL spectra of PQDs over different times at 70 °C in solution.

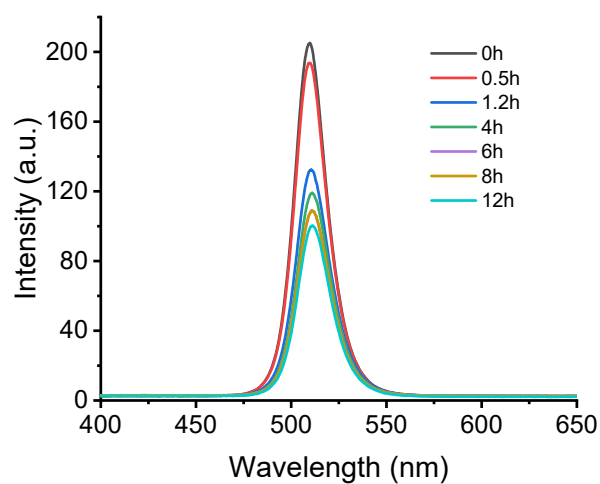


Figure S29. PL spectra of F-PQDs over different times at 70 °C in solution.

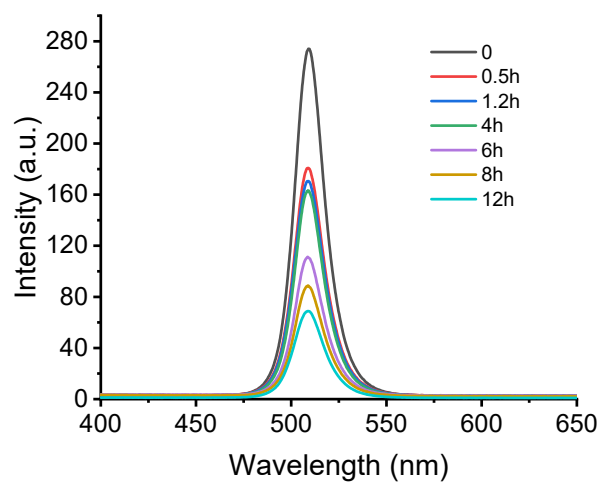


Figure S30. PL spectra of POEGMA₇₈-b-PFOEMA₃₄ hybrid nano assemblies over different times at 70 °C in solution.

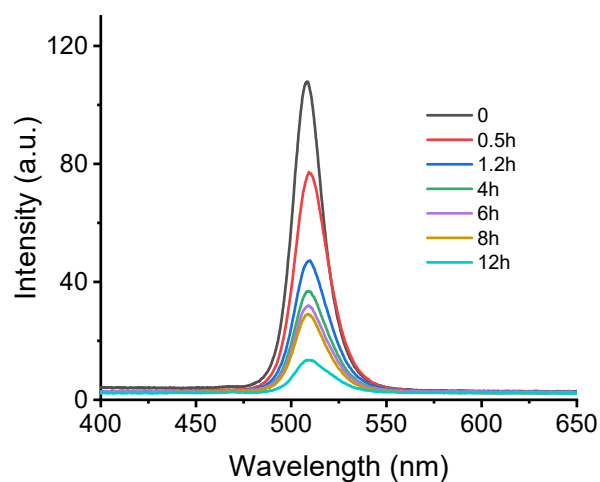


Figure S31. PL spectra of POEGMA₇₈-b-PFOEMA₇₅ hybrid nano assemblies over different times at 70 °C in solution.

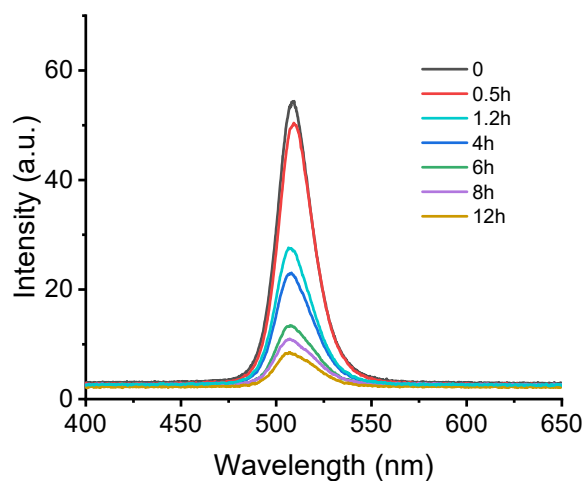


Figure S32. PL spectra of POEGMA₇₈-b-PFOEMA₁₃₇ hybrid nano assemblies over different times at 70 °C in solution.

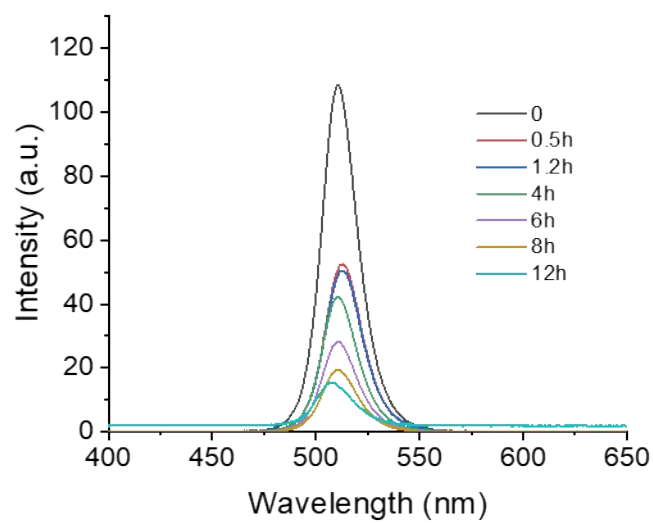


Figure S33. PL spectra of POEGMA₇₈-b-PFOEMA₂₁₅ hybrid nano assemblies over different times at 70 °C in solution.

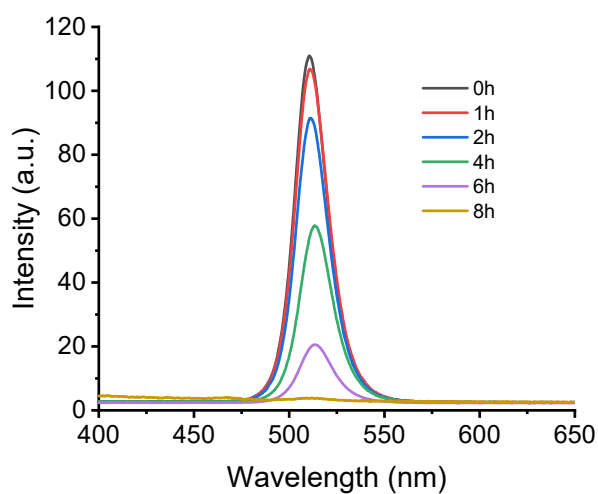


Figure S34. PL spectra of PQDs over different times against UV light irradiation in solution.

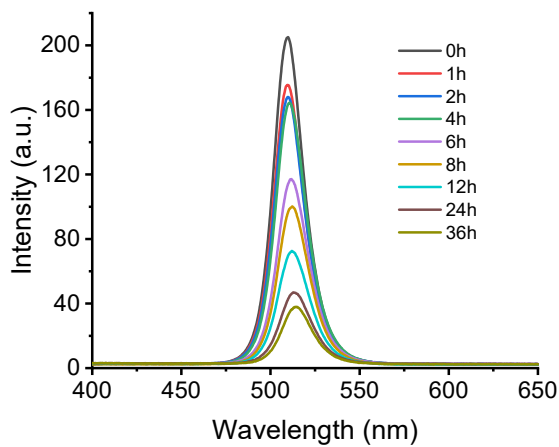


Figure S35. PL spectra of F-PQDs over different times against UV light irradiation in solution.

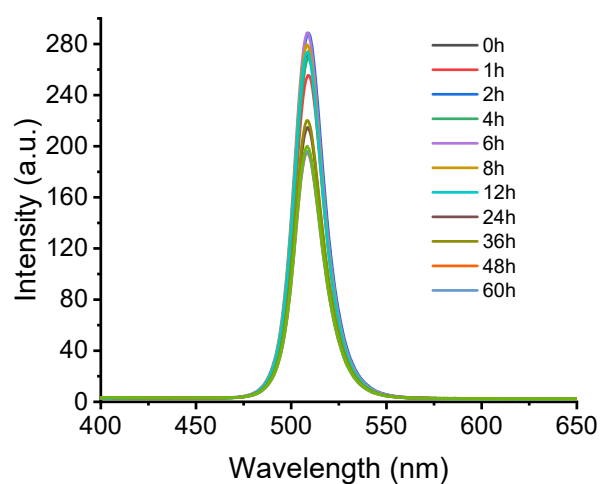


Figure S36. PL spectra of POEGMA₇₈-b-PFOEMA₃₄ hybrid nano assemblies over different times against UV light irradiation in solution.

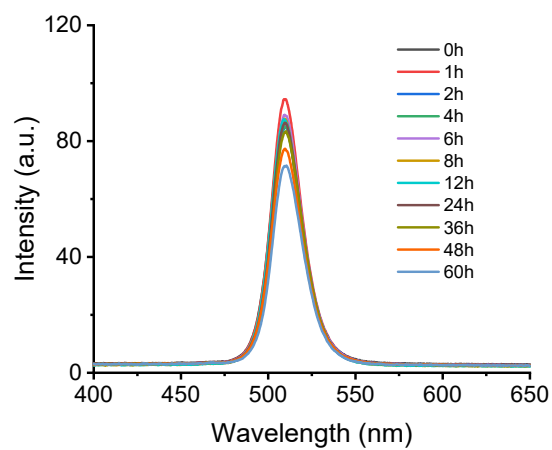


Figure S37. PL spectra of POEGMA₇₈-b-PFOEMA₇₅ hybrid nano assemblies over different times against UV light irradiation in solution.

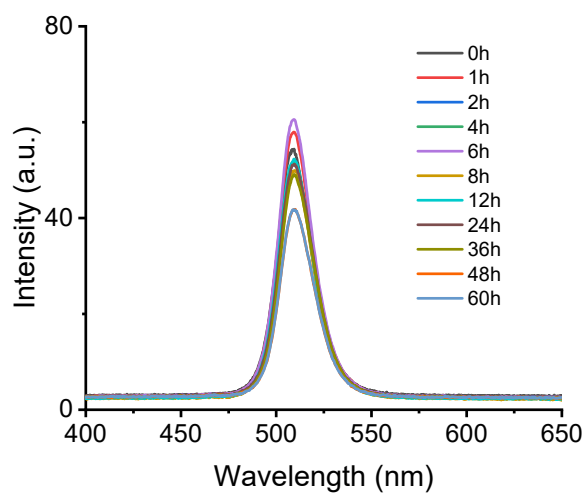


Figure S38. PL spectra of POEGMA₇₈-b-PFOEMA₁₃₇ hybrid nano assemblies over different times against UV light irradiation in solution.

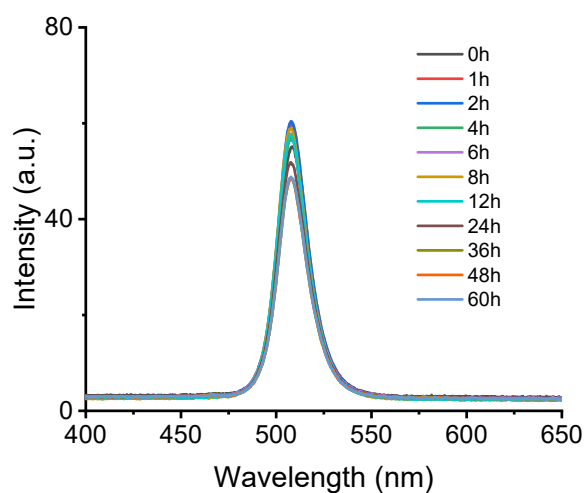


Figure S39. PL spectra of POEGMA₇₈-b-PFOEMA₂₁₅ hybrid nano assemblies over different times against UV light irradiation in solution.

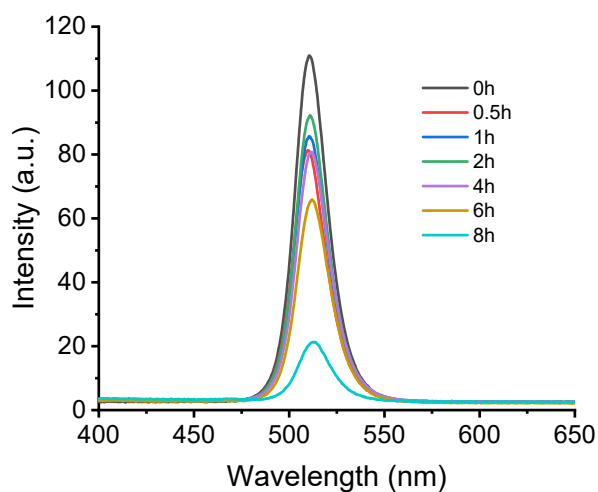


Figure S40. PL spectra of PQDs over different times in solution upon mixing with isopropanol.

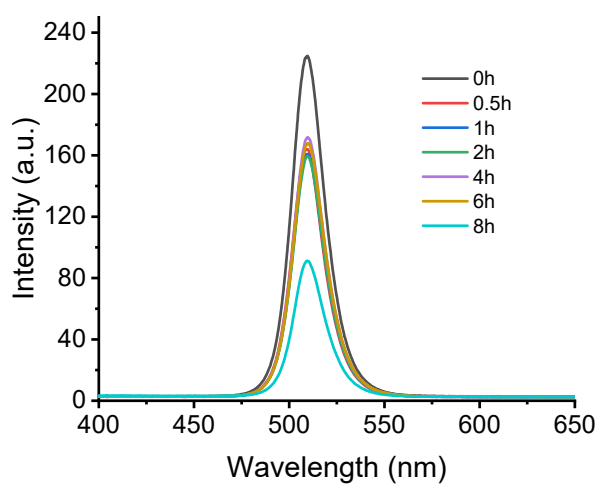


Figure S41. PL spectra of F-PQDs over different times in solution upon mixing with isopropanol.

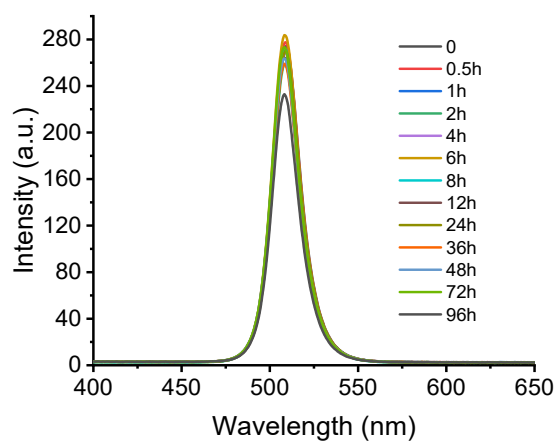


Figure S42. PL spectra of POEGMA₇₈-b-PFOEMA₃₄ hybrid nano assemblies over different times in solution upon mixing with isopropanol.

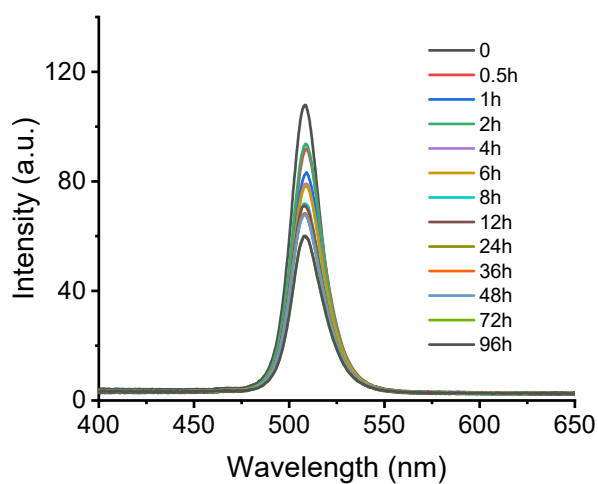


Figure S43. PL spectra of POEGMA₇₈-b-PFOEMA₇₅ hybrid nano assemblies over different times in solution upon mixing with isopropanol.

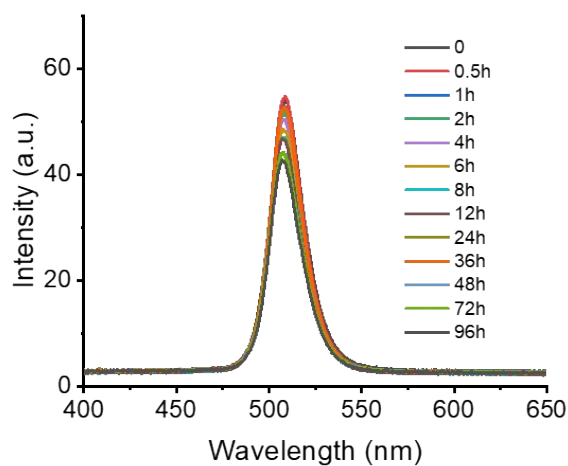


Figure S44. PL spectra of POEGMA₇₈-b-PFOEMA₁₃₇ hybrid nano assemblies over different times in solution upon mixing with isopropanol.

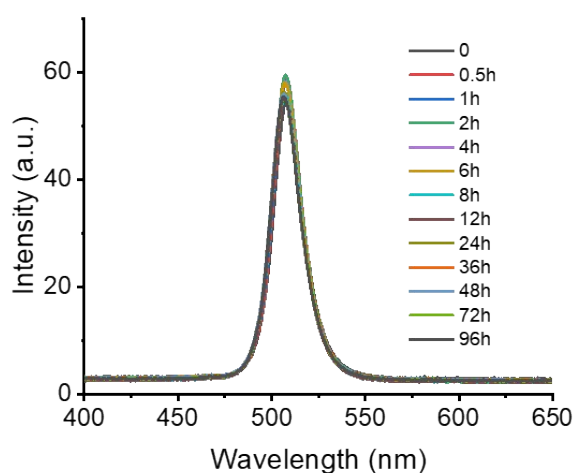


Figure S45. PL spectra of POEGMA₇₈-b-PFOEMA₂₁₅ hybrid nano assemblies over different times in solution upon mixing with isopropanol.

References

- [1] K. Chen, X. Deng, G. Dodekatos and H. Tuysuz, Photocatalytic polymerization of 3,4-ethylenedioxythiophene over cesium lead iodide perovskite quantum dots. *J. Am. Chem. Soc.*, 2017, **139**, 12267-12273.
- [2] Y. C. Wong, J. De Andrew Ng and Z. K. Tan, Perovskite-initiated photopolymerization for singly dispersed luminescent nanocomposites. *Adv. Mater.*, 2018, **30**, 1800774.
- [3] Y. Zhu, Y. Liu, K. A. Miller, H. Zhu and E. Egap, Lead halide perovskite nanocrystals as photocatalysts for PET-RAFT polymerization under visible and near-infrared irradiation. *ACS Macro Lett.*, 2020, **9**, 725-730.
- [4] S. Liang, S. He, M. Zhang, Y. Yan, T. Jin, T. Lian and Z. Lin, Tailoring charge separation at meticulously engineered conjugated polymer/perovskite quantum dot interface for photocatalyzing atom transfer radical polymerization. *J. Am. Chem. Soc.*, 2022, **144**, 12901-12914.

- [5] X. Jin, K. Ma, J. Chakkamalayath, J. Morsby and H. Gao, In situ photocatalyzed polymerization to stabilize perovskite nanocrystals in protic solvents. *ACS Energy Lett.*, 2022, **7**, 610-616.
- [6] X. Jin, K. Ma and H. Gao, Tunable luminescence and enhanced polar solvent resistance of perovskite nanocrystals achieved by surface-initiated photopolymerization. *J. Am. Chem. Soc.*, 2022, **144**, 20411-20420.
- [7] C. Zhao, H. Song, Y. Chen, W. Xiong, M. Hu, Y. Wu, Y. Zhang, L. He, Y. Liu and A. Pan, Stable and recyclable photocatalysts of CsPbBr₃@MSNs nanocomposites for photoinduced electron transfer RAFT polymerization. *ACS Energy Lett.*, 2022, **7**, 4389-4397.
- [8] Y. Zhu, Y. Liu, Q. Ai, G. Gao, L. Yuan, Q. Fang, X. Tian, X. Zhang, E. Egap, P. M. Ajayan and J. Lou, In situ synthesis of lead-free halide perovskite-COF nanocomposites as photocatalysts for photoinduced polymerization in both organic and aqueous phases. *ACS Mater. Lett.*, 2022, **4**, 464-471.
- [9] Z. Xia, B. Shi, W. Zhu, Y. Xiao and C. Lü, Binary hybridization strategy toward stable porphyrinic Zr-MOF encapsulated perovskites as high-performance heterogeneous photocatalysts for red to NIR light-Induced PET-RAFT polymerization. *Adv. Funct. Mater.*, 2022, **32**, 2207655.
- [10] H. Zhu, M. Cheng, J. Li, S. Yang, X. Tao, Y. Yu and Y. Jiang, Independent dispersed and highly water-oxygen environment stable FAPbBr₃ QDs-polymer composite for down-conversion display films. *Chem. Eng. J.*, 2022, **428**, 130974.
- [11] L. Protesescu, S. Yakunin, M. I. Bodnarchuk, F. Krieg, R. Caputo, C. H. Hendon, R. X. Yang, A. Walsh and M. V. Kovalenko, Nanocrystals of cesium lead halide perovskites (CsPbX₃, X = Cl, Br, and I): novel optoelectronic materials showing bright emission with wide color gamut. *Nano Lett.*, 2015, **15**, 3692-3696.
- [12] D. Sato, Y. Iso and T. Isobe, Effective stabilization of perovskite cesium lead bromide nanocrystals through facile surface modification by perfluorocarbon acid. *ACS Omega*, 2020, **5**, 1178-1187.